Top-down and sensitive indium oxide nanoribbon field effect transistor biosensor chips integrated with on-chip gate electrodes toward point of care applications

To cite this article before publication: Noppadol Aroonyadet *et al* 2018 *Nanotechnology* in press https://doi.org/10.1088/1361-6528/aad435

Top-down and sensitive indium oxide nanoribbon field effect transistor biosensor chips integrated with on-chip gate electrodes toward point of care applications

N. Aroonyadet[1,*], W. Jeamsaksiri[2], A.Wisitsoraat[2], A. Tuantranont[2]

[1]National Nanotechnology Center, 111 Thailand Science Park, Phahonyothin Road, Khlong Nueng Khlong Luang, Pathum Thani 12120, THAILAND

[2]National Electronic and Computer Technology Center, 112 Thailand Science Park, Phahonyothin Road, Khlong Nueng Khlong Luang, Pathum Thani 12120, THAILAND

E-mail: noppadol@nanotec.or.th

Abstract:

We report a scalable, uniform, and sensitive top-down fabricated indium oxide (In_2O_3) nanoribbon biosensor platform with integrated on-chip gate electrodes using two photolithographic masks. The purpose of this on-chip gate electrode is to control the operational point of the sensor during biomolecular detection replacing the cumbersome external Ag/AgCl electrode. It exhibits excellent capability in gating transistors in an aqueous condition and high stability during the sensing experiment, which is similar to the Ag/AgCl electrode. Its compactness increases the portability and pushes this platform toward a practical use. To demonstrate its capability for detection of biomolecules, we combine this platform with the electronic enzyme-linked immunosorbent assay (ELISA) technique to amplify the signal and to bypass limitation of the Debye screening effect from high salt concentration of physiological samples. Troponin I, a cardiac marker for diagnosis of acute myocardial infarction (AMI), was selected as the target molecule in this study. The In_2O_3 nanoribbon device offers a high

response of 30% toward 0.1 pg/mL troponin I concentration and a lower detection limit than that of the commercial ELISA kit on the market by 5 orders of magnitude. The total assay time from the sample collection to the data acquisition is about 45 minutes, which is within the constraint of the emergency care application. With the demonstrated sensitivity, uniformity, scalability, quick turn-around time and ability to be integrated, our In_2O_3 nanoribbon biosensor platform has high potential toward clinical tests for early diagnosis of AMI.

Keywords: nanoribbon biosensor, on-chip gate electrode, FET biosensor, In_2O_3 nanoribbon

1. Introduction

Field effect transistor (FET) based sensors constructed from nanomaterials have drawn great attentions from researchers due to their promising performance for biological and chemical detections [1]. Benefits inherited from nanomaterials utilized as active channels of transistors include their tremendous surface to volume ratio and their comparable dimension to target molecules contributing to their high sensitivity [1]. Wide varieties of species such as proteins [2], viruses [3], DNA strands [4], and chemical species [1] have been detected at extremely low concentrations by nanomaterial-based FET sensors. Although FET biosensors fabricated from bottom-up nanomaterials (nanowires [1] or nanotubes [5] etc.) are very sensitive, they face challenges in the device fabrication and uniformity in their performance. To overcome these challenges, an alternative "top-down" approach has been proposed to construct devices from ultrathin silicon on insulator (SOI) wafers to be restricted in the same dimension as the bottom up one [6]. Recently, a concept of nanoribbon FET biosensors of which the lateral dimension is the key factor to determine sensitivity has been proposed. This concept allows a relatively simple fabrication process with conventional facilities [7]. To lower the device cost, metal oxide nanoribbon FET biosensors have been demonstrated with good device uniformity and sensitivity to protein biomarkers [8, 9]. Another key element for FET based biosensors is the gate electrode necessary for tuning the operational point to achieve the ultimate sensitivity. Several types of gate electrodes were used to adjust a device working mode such as platinum, Ag/AgCl [5, 10], or a conductive substrate [7]. The platinum gate electrode confronts instability in controlling electrical

potential during sensing experiment due to protein binding on its surface [10]. To use conductive substrate as the gate electrode, additional steps and lithographic masks for the device fabrication are needed to create the connection between the electrode pad and the substrate, limiting the choice of the substrate material. The Ag/AgCl electrode has been widely used as the reference electrode due to its long-proven potential stability in electrochemical experiments [10]. Integrating this electrode into the conventional fabrication process is challenging due to restriction of applicable materials in microelectronic facilities. In addition, the Ag/AgCl electrode needs to be submerged in 3 M potassium chloride solution to stabilize chloride concentration and to prevent corrosion of the electrode, obstructing its seamless integration into a FET structure.

Over a million of people visit the emergency department every year due to their chest pain or other symptoms, which are sign of acute coronary syndrome (ACS) and about 10% of these patients experience acute myocardial infarction (AMI) [11]. Myocardial infarction is one of major emergency diseases in the United States and around the globe. In the medical facility, the diagnosis of myocardial infarction relies on electrocardiogram (ECG) to record electrical activities of heart via electrodes attached on the patient's skin. ECG can identify the damaged area due to the abnormality of electrical signals for quick assessment in the emergency department. However, ECG has significant limitations that it is unable to quantify severity of heart damage and it falsely shows normal electrical patterns from 50 % of ACS patients [12]. In addition to diagnosis with ECG, the blood flow of suspected AMI patients must be monitored in order to detect any clot in their blood vessels using dye or radioactive substances combined with an imaging technique. Medical staffs need to gather quick, correct and comprehensive information in order to identify the disease of the patient, to evaluate its severity and to provide proper treatment for that patient. Therefore, patients are usually diagnosed to be AMI based on 2 of 3 indicators including typical symptoms of AMI, Q wave patterns from ECG and blood test results from the medical laboratory [11]. Troponin, a complex regulatory protein found in cardiac muscle, has 3 isoforms including C (the calcium binding component), T (the tropomyosin binding component) and I (the inhibitory component). Troponin I and T, which have sufficient identity to allow production of their antibodies, are normally released to blood stream due to the death of cardiac muscle cells;

therefore, troponin I and T are not in the blood of healthy people [11]. Levels of both troponin isoforms increase within 4 to 9 hours and peak at 12 to 24 hours after AMI [11]. However, the detection of cardiac biomarkers using the conventional ELISA approach requires costly instruments, well-trained staffs to conduct the test and a well-equipped medical laboratory. In addition, the detection limit of commercial gold standard troponin ELISA kits is 6 pg/mL, which is insufficient for early diagnosis for AMI [13]. Several approaches have been proposed by many researchers to simplify the blood test for diagnosis of AMI and to enhance sensitivity toward key biomarkers for early detection of AMI. For instance, bottom-up-synthesized polyaniline nanowire biosensors have been demonstrated to detect myoglobin, troponin I, CK-MB and BNP in diluted phosphate buffer saline (PBS) [14]. Also, top-down-fabricated silicon nanowire biosensors were utilized to detect troponin T [15-17], troponin I [13], CK-MM [17], and CK-MB [17]. However, these approaches require complicated sample preparation process to lower salt concentration in order to alleviate the Debye screening effect of the transistor [15, 16].

Herein, we propose a new biosensor platform based on top-down-fabricated indium oxide (In_2O_3) nanoribbons with an alternative integrated gate electrode that can be accomplished with a few fabrication steps. The proposed on-chip gate electrode is compared with the Ag/AgCl electrode in term of electrical and sensing performances. In addition, an alternative approach to functionalize surface of In_2O_3 nanoribbons based on silane chemistry is systematically investigated in order to improve the immobilization of probe molecules and increase the specificity of biosensors toward target molecules. The incubation time and concentration of silane cross-linked chemistry are adjusted to yield the maximum surface coverage. Biotin molecules are anchored on the metal oxide surface and streptavidin tagged with red fluorescent dye is introduced to validate this surface functionalization. To demonstrate a possible point-of-care application, we select troponin I, a Food and Drug Administration of United States (US FDA) approved cardiac biomarker, as a model protein for diagnosis AMI using the proposed biosensor chip. We demonstrated that troponin I could be detected at 0.1 pg/mL with a projected limit of detection about 5 orders of magnitude lower than that of the commercial ELISA kit.

2. Experimental details

2.1 Device fabrication

In this study, FET based biosensor chips were fabricated using conventional microelectronic fabrication facilities. Firstly, 300 nm silicon nitride (Si_3N_4) film was deposited on silicon wafers (University Wafer, USA); then, they were patterned with two photolithographic masks for metal and metal oxide nanoribbon deposition. Layers of titanium/gold/titanium (Ti/Au/Ti) (Kurt J Lesker, USA) were deposited as source, drain and on-chip metal gate electrodes by a radio frequency (RF) sputtering technique. Secondly, In_2O_3 nanoribbons were formed by resist patterning and lift-off processes in order to obtain a clean ribbon surface for surface functionalization. Deposition time for indium oxide (Kurt J Lesker, USA) sputtering was controlled to obtain the film thickness of 23 nm within the transistor Debye's length [8] as shown in Figure 1. The schematic diagram of a FET device in Figure 1 (a) depicts source and drain Ti/Au electrodes with a top TiO_2 passivation layer to minimize leakage current during sensing experiments. A nanoribbon was bridged between these electrodes. Electrical pads were finally exposed by dipping in basic piranha solution after deposition and lifting of unwanted metal oxide area. Figure 1b-1 shows an optical image of a biosensor chip cut from a 3-inch fabricated silicon wafer (Figure 1b-2). Each chip consists of six transistors and two identical on-chip gate electrodes for redundancy as shown in Figure 1b-3. Figure 1b-4 is a photograph of two identical nanoribbons to exemplify the reproducibility of the top-down fabrication approach. The structural consistency provides the uniformity in electrical characteristics, allowing the simple interpretation of the detected sensing response to a biomarker concentration in a sample solution. Additionally, its fabrication scalability helps to lower the cost of sensors [8].

2.2 Electrical characterization

An as-fabricated In_2O_3 nanoribbon FET chip was placed onto a chip tray of the test fixture as shown in Figure 1c-1 before inserting the tray under a taper-shape Teflon chamber and pressing both clamps down to confine the sample solution during sensing experiments (Figure 1c-2). Figure 1c-3 displays a top-view photograph of the test fixture with the 2 mm opening on the active area of transistors. We added 200 μL of 100 times dilution of 10 mM phosphate buffer saline (1xPBS)

(pH = 7.4) or 0.01x PBS (Sigma Aldrich, USA) in the sensing chamber before electrical measurements using a Keysight B1500A semiconductor analyzer (Keysight, USA).

2.3 Ionic sensitivity test

An as-fabricated chip was mounted into the test fixture and connected to the semiconductor analyzer to monitor 3 devices simultaneously. The biosensor chip was biased via the on-chip gate electrode and the commercial Ag/AgCl electrode for the comparison of their ionic sensitivity. We filled 200 μL of commercial pH buffer solution (Carlo Erba, France) with different pH ranging from pH 9.0 to pH 4.0 into the sensing chamber and replaced manually with a pipet.

2.4 Optimization of carboxyethylsilanetriol surface chemistry

The carboxyethylsilanetriol (CBES) (Gelest, USA) surface chemistry was evaluated using electrochemical impedance spectroscopy (EIS) in order to optimize the surface coverage, chemical concentration and incubation time of the sample in the linker molecule solution to maximize binding sites of probe molecules, which would increase a chance to capture target molecules and the sensitivity of sensors [18]. Indium doped tin oxide (ITO) substrates were cleaned with acetone, isopropyl alcohol and deionized water before blowing dry with nitrogen stream. After that, ITO substrates were treated with oxygen plasma at power equally to 30 W and pressure of 400 mTorr for 1 minute and then incubated in 0.1, 1, 10, and 14.91 mM (1% v/v) CBES solution with varying times from 30 minutes to 24 hours. In EIS measurement, 100 mM phosphate buffer pH 7.4 was prepared from disodium phosphate (Na_2HPO_4) (Sigma Aldrich, USA) and monosodium phosphate (NaH_2PO_4) (Sigma Aldrich, USA) with 1 mM potassium ferricyanide ($K_3Fe(CN)_6$) (Sigma Aldrich, USA) and 1 mM potassium ferrocyanide ($K_4Fe(CN)_6$) (Sigma Aldrich, USA). Substrates were immersed into 10 mL of the solution with the exposed area of 0.5 cm^2 and the biased at potential = 0.190 V superimposed by an alternating current (AC) amplitude of 5 mV in the frequency ranging from 0.01 Hz to 10 kHz (CHI660D, CH Instruments, USA).

2.5 Fluorescent experiment for verification of CBES surface chemistry

In order to validate the surface coverage of linker molecules, sputtered In_2O_3 film on silicon substrates were functionalized with 1% v/v CBES for 1 hour. After immobilization of CBES molecules, carboxylic terminals of CBES linker molecules on the indium oxide film were activated with the mixture of 20 mM N-(3-Dimethylaminopropyl)-N-ethylcarbodiimide hydrochloride (EDC) (Sigma Aldrich, USA) and 20 mM N-Hydroxysulfosuccinimide sodium salt (Sulfo-NHS) (Sigma Aldrich, USA) for 30 minutes to prepare for covalently coupling between amine terminal molecules and the linker molecule similar to the previous work [8]. Next, the activated substrates were submersed into the sample solution containing 5 mM amine-PEG2 biotin (Thermo Scientific, USA) in 10 mM PBS (1x PBS), pH 7.4 and into the negative control solution comprising of 5 mM amine poly (ethylene glycol) (PEG) (Laysan Bio, USA) in 1x PBS pH 7.4 for 1 hour before rinsing off unbound molecules by wash buffer (0.05% v/v Tween 20 (Sigma Aldrich, USA) in 1x PBS pH 7.4). After that, the solution of 1 μM streptavidin tagged with fluorescent red dye (Invitrogen, USA) was dropped onto both substrates and incubated for 1 hour before rinsing with the wash buffer and deionized water. Lastly, both substrates were inspected with a fluorescent microscope (Olympus BX53, Japan).

2.6 Functionalization of In_2O_3 nanoribbon FET chips for the detection of troponin I protein

To enable the nanoribbon FET functional as the biosensor, a FET chip was functionalized with 1 % v/v of CBES solution for 1 hour to anchor linker molecules with the carboxylic terminal for coupling with the capture probe molecules as the protocol mentioned in section 2.4. After immobilization of CBES linker molecules, 10 μL of 200 μg/mL troponin I antibody solution (Fitzgerlad Industry, USA) was dropped on the transistor channel area to bind with the linker molecule through the EDC/NHS chemistry for 3 hours at room temperature. After immobilization of capture antibodies, the sensor surface were treated by 10 μL of 2% w/v bovine serum albumin (BSA) (Sigma Aldrich, USA) in wash buffer for 30 minutes to block unspecific binding of biomolecules. After removal of blocking solution, sensors were incubated with 10 μL of troponin I protein solution for 10 minutes at room temperature. After protein incubation, excess proteins were rinsed off by wash buffer and PBS solution 3 times. Next, devices were soaked in 10 μL of

100 μg/mL biotinylated troponin I antibody solution (Fitzgerlad Industry, USA) for 10 minutes at room temperature before rinsing off the unbound antibody. After that, 10 μL of 10 nM streptavidin solution was introduced into the sensing chamber and allowed to react with biotinylated antibodies for 5 minutes to provide binding sites for biotinylated urease enzymes before rinsing off the excess protein. Finally, devices were incubated with 10 μL of 100 μg/mL of biotinylated urease enzymes solution (Genetex, USA) for 10 minutes before washing away unreacted enzymes.

3. Results and discussion

3.1 Electrical characterization

The electrical performances of fabricated devices were characterized using a Keysight B1500 semiconductor analyzer. In biosensing experiments, devices were immersed in an electrolyte solution and controlled by the gate electrode to tune their operational point into subthreshold regime to achieve their optimum performance [19]. To benchmark the utilization of different gate electrodes, electrical characterization was performed in 0.01x PBS to lower ionic concentration in the electrolyte in order to alleviate the Debye's screening effect [4]. Devices were biased by a commercial Ag/AgCl electrode (eDAQ, Australia) and our proposed on-chip gate electrode. Figure 2.1 (a) depicts a schematic diagram of the liquid gating measurement. Potential was applied through the gate electrode to extract electrical characteristics and another external Ag/AgCl electrode was inserted to measure the effective liquid gate potential relative to channels of transistors in the electrolyte. The change in current of the transistor biased with the on-chip gate electrode was found to be similar to the same transistor biased with the Ag/AgCl electrode when the effective gate potential varied from -1.5 to 1.5 V as shown in Figure 2 (b). This result indicates that the on-chip gate electrode can control transistors to achieve nearly the same result as the commercial Ag/AgCl electrode. At the same liquid gate potential of 1.20 V and drain voltage (V_{DS}) of 200 mV, the on-state current (I_{ON}) of the device was equal to 8.89 μA and 9.17 μA when the bias voltages (V_{GS}) were applied through the Ag/AgCl electrode and the on-chip gate electrode, respectively, The on state to off state current ratio (on/off) and transconductance (g_M) extracted from the I_{DS}-V_{GS} curve with the applied voltage through the Ag/AgCl electrode were 3.19×10^4 and

9.89 μS while those parameters derived from the I_{DS}-V_{GS} curve with the on-chip gate electrode configuration were 6.33×10^4 and 8.04 μS, respectively. Figure 2 (c) shows family curves of drain current (I_{DS}) versus drain voltage (V_{DS}) of an In_2O_3 nanoribbon device when it was biased via an on-chip gate electrode. Our nanoribbon device exhibited a good metal oxide semiconductor field effect transistor (MOSFET) behavior where I_{DS} varied linearly with V_{DS} and saturated at the voltage higher than 1 V. From Figure 2 (b) and (c), the nanoribbon device shows n-channel transistor behavior in which the drain current decreases when the gate potential is reduced and the device is turned off when the gate potential goes below 0 V.

3.2 Ionic sensitivity test

After obtaining devices with proper electrical performances in the electrolyte, the ionic sensitivity of devices was verified using the pH sensing experiment to ensure that devices biased by the on-chip gate electrode were suitable for biosensing applications and had enough ionic sensitivity. Both types of gate electrodes were applied to tune the operational point of devices into subthreshold regime to maximize device sensitivity. Figure 2 (c) shows the average of normalized pH sensing responses from three devices biased by the Ag/AgCl and the on-chip gate electrodes when pH of the buffer solution in the sensing chamber changed from pH 4 to pH 9. We found that pH response of devices biased by either Ag/AgCl or on-chip gate electrodes decreased when pH of buffer solution in the sensing chamber increased. This behavior was due to decrease in hydrogen ions in solution resulting in the reduction of modulated gate potential. For n-type indium oxide nanoribbon devices, the drain current also decreases when the gate potential reduce. Responses from devices biased via the Ag/AgCl electrode changed from 1 to 49.19 times when pH of the solution in the sensing chamber reduced from 9 to 4. Similarly, responses from devices controlled by the on-chip gate electrode altered from 1 to 43.15 with the same pH variation. From this experiment, we demonstrated that the proposed integrated gate electrode could be applied for sensing experiments with comparable sensing performances to the commercial Ag/AgCl electrode.

3.3 Surface chemistry investigation

Specificity is one of the most important properties of biosensors. To transform transistors to specific sensors, probe molecules bound to their target molecules (e.g. proteins, antibodies, deoxyribonucleic acid (DNA) strands, or ribonucleic acid (RNA) strands etc.) were selectively immobilized on the surface of an active transistor channel. Typically, indium oxide nanoribbons were gradually etched by 3-phosponopropionic acid (PPA) during the incubation to immobilize PPA molecules on the indium oxide nanoribbon surfaces [8]. Nanoribbons were etched about 17 nm for incubation time of 5 hours and 30 minutes measured by an atomic force microscope (Seiko SPA300, Japan). Therefore, the incubation time of indium oxide nanoribbons in PPA solution needed to be carefully controlled although etching of indium oxide out of nanoribbon surface helps to gain more pristine surface for coupling with linker molecules. To avoid etching of In_2O_3 nanoribbons, an alternative chemistry to PPA was proposed to be CBES to cross-link between hydroxyl terminals on the metal oxide surface and ones of CBES. Figure 3 (a) shows a molecular structure of CBES. It has hydroxyl terminals similar to ones in PPA. Figure 3 (b) shows schematic diagrams of CBES immobilization on the indium oxide surface. After cleaning the indium oxide surface, the substrate was treated with oxygen plasma to introduce more hydroxyl groups on the surface in addition to intrinsic hydroxyl groups causing by dangling bond of metal oxide. To optimize the incubation time and concentration of CBES, ITO substrates were incubated in 0.1 mM, 1 mM, 10 mM and 14.91 mM or 1% v/v CBES solution to anchor CBES linker molecules on the oxide surface with varying times from 30 minutes to 24 hours. The sample impedance was measured by the EIS technique. The surface coverage (θ) was calculated from $1-R_{Bare}/R_{SAM}$ where R_{Bare} and R_{SAM} are radii of fitted curves from the EIS results of a bare ITO substrate and ITO substrates immersed in CBES solution at different CBES concentration and incubation times, respectively. The computed surface coverage are shown in Figure 3 (c). The surface coverage of 0.1 mM CBES concentration seems to reach its maximum value at about 70% since 1 hour of incubation. It remains at the same level even though the incubation time increases further to 24 hours. At a higher CBES concentration of 1 mM, the saturated level increases to 90% after incubating in the solution for 7 hours and maintains at that level up to the incubation time of 24 hours. With the CBES concentration of 10 mM, 90% coverage was achieved after incubating the

ITO substrate for 5 hours and the surface coverage slightly increased to 92% after increasing the incubation time up to 24 hours. For the CBES concentration of 14.91 mM or 1% v/v, more than 95% coverage was attained when the substrate was immersed in CBES solution for more than 1 hour and remained at this level even though the sample was soaked in the solution up to 24 hours. This observation was similar to the study result of PPA surface chemistry reported previously [18]. To visually confirm the surface coverage of CBES molecules, a fluorescent experiment was performed on the sputtered In_2O_3 film on silicon substrate having the same thickness as nanoribbons as illustrated in schematic diagrams (Figure 3 (d) and (e)) and described earlier in the experimental section. Biotin was chosen due to its high affinity to a streptavidin molecule while PEG molecules cannot capture any streptavidin molecule, which would be washed away during the rinsing step. Fluorescent photographs were taken from the sample and its negative control substrates using a fluorescent microscope as shown in Figure 3 (f) and (g), respectively. A uniform red fluorescent signal was obtained from the sample substrate demonstrating that streptavidin tagged with red fluorescent dyes were evenly immobilized on the surface of the sample substrate via the biotin capture probe. It also confirms the high and uniform surface coverage of CBES linker molecules. In contrast, a dark image was obtained from the negative control due to the fact that streptavidin molecules could not bind to PEG molecules on the surface of the control substrate and were washed away.

3.4 Sensing experiment of troponin I protein

After confirming that the FET devices with the integrated on-chip gate electrode exhibit good electrical performance and high ionic sensitivity, troponin I, a cardiac biomarker for AMI diagnosis, was selected as a model protein to evaluate their biosensing performances. Figure 4 (a) shows schematic diagrams of surface modification of an In_2O_3 nanoribbon FET chip for troponin I detection by the electronic ELISA technique as described earlier in Section 2.6. The advantages of electronic ELISA are that we can circumvent the Debye screening effect from sensing of FET biosensors in the physiological solution due to high salt concentration and enable this platform to directly deal with the physiological solution without any complicated sample preparation. In

addition, the sensing signal can be amplified by enzyme activities leading to lower the limit of detection (LOD) [4, 8, 20]. A change in conduction of In_2O_3 nanoribbon FET devices can be correlated to the alteration of pH in the sensing chamber from a reaction of urease enzymes immobilized on target molecules and urea solution in the sensing chamber.

$$\text{Urea} + 2H_2O + H^+ \xrightarrow{\text{Urease}} 2NH_4^+ + HCO_3^-$$

Figure 4 (b) shows normalized real-time responses from three nanoribbon devices after the immobilization of streptavidin as a control experiment for troponin I detection. Devices were initially immersed in 200 μL of 0.01x PBS with pH 7.4 and we replaced 0.01xPBS solution in the sensing chamber with 200 μL of 10 mM urea in 0.01x PBS with pH 6.59. Conduction of devices was decreased due to increasing pH in the sensing chamber, which yielded positive gating on n-type nanoribbon transistors. After the control experiment, devices were rinsed with 1xPBS before they were incubated in biotinylated urease enzyme at room temperature to immobilize urease enzymes on the sensor surface. The number of bound enzymes on the surface of nanoribbons corresponds to the number of captured target molecules. To perform the electronic ELISA, devices were initially immersed in 200 μL of 0.01x PBS with pH 7.4 before the 0.01x PBS solution in the sensing chamber was manually exchanged with 200 μL of 10 mM Urea in 0.01xPBS. Figure 4 (c) demonstrates normalized real-time sensing responses from three nanoribbon sensors monitored simultaneously for the detection of troponin I protein at 300 pg/mL concentration. The average normalized currents of all three sensors reduced about 82 % from the base line current due to the hydrolysis reaction between urea and urease enzymes causing an increase in pH in the sensing chamber from 7.40 to 8.85. The hydrolysis reaction deprotonates hydrogen ions out from hydroxyl groups on the surface of nanoribbons resulting in negative gating effect for n-type In_2O_3 nanoribbon FETs. The total assay time was about 45 minutes after introducing the target protein solution until getting the sensing result. After the detection of troponin I at 300 pg/mL, similar sensing experiments were repeated for other troponin I concentrations including 10, 1 and 0.1 pg/mL. Figure 4 (d) shows the average normalized responses for various troponin I concentrations.

Each data point was calculated from three sensors monitored concurrently during the experiment. The sensing response decreases exponentially upon decreasing concentration of troponin I target molecules. A blank sample was also performed to calculate limit of blank, but the increasing response similar to Figure 4 (b) was obtained due to the absence of troponin I protein in the solution. Using the equation from its fitting curve in Figure 4 (d), the projected limit of detection with 1% response is about 15 ag/mL, which is about 5 orders of magnitude lower than that of the commercial ELISA [13]. For patients with acute myocardial infarction, the level of troponin I is elevated due to release of troponin proteins from the death of cardiac myocytes. The clinically relevant level for troponin I is about 40 pg/mL [21]. Any detectable level of troponin I is a sign of myocardial infarction and severity depends on concentration of troponin I protein because troponin is not present in healthy people [11]. Thus, the lower detection limit of troponin I will allow the earlier diagnosis of AMI, beneficial to reducing rate of mortality as a physician can provide a proper treatment to an AMI patient upon the detection.

4. Conclusions

In summary, we demonstrated fabrication processes of highly scalable top-down In_2O_3 nanoribbon biosensor chips with integration of on-chip gate electrode using two simple photolithographic masks to define position and dimension of metal electrodes and nanoribbons. The Ti/Au/Ti on-chip gate electrode showed comparable gating performance to the commercial Ag/AgCl electrode at the same liquid gate potential. Moreover, In_2O_3 nanoribbon devices show uniform electrical characteristics in the aqueous condition when the gate voltage is applied through the on-chip gate electrode. In addition, In_2O_3 nanoribbon devices with the on-chip gate electrode offered good ionic sensitivity with 45 times decrease in conduction when pH was increased from 4 to 9. Furthermore, the electronic ELISA detection of troponin I yielded an average response of 30% at 0.1 pg/mL troponin I, which was about two orders of magnitudes lower than the clinically relevant level. Also, the assay time was reduced to be about 45 minutes, which is short enough for the practical use without a significant loss of sensitivity. Nevertheless, further investigations of optimization of the assay time and more statistical study with real patients' samples or spiked target

proteins in physiological samples are needed to confirm the validity of the proposed biosensor for the point of care application.

5. Acknowledgements

We would like to thank Thai Microelectronics Center, National Electronic and Computer Technology Center, NSTDA Characterization and Testing Center for device fabrication and characterization. We are grateful to Professor Supapan Seraphin for her helps and valuable comments. This study was financially supported by the Thailand Research Fund (TRG5980010) and National Nanotechnology Center (P-1651165).

6. References

1. Cui, Y., et al., *Nanowire nanosensors for highly sensitive and selective detection of biological and chemical species.* Science, 2001. **293**(5533): p. 1289-1292.
2. Zheng, G.F., F. Patolsky, and C.M. Lieber, *Multiplexed electrical detection of cancer marker proteins and single viruses by nanowire fet arrays.* Abstracts of Papers of the American Chemical Society, 2005. **229**: p. U782-U782.
3. Patolsky, F., et al., *Electrical detection of single viruses.* Proceedings of the National Academy of Sciences of the United States of America, 2004. **101**(39): p. 14017-14022.
4. Stern, E., et al., *Importance of the debye screening length on nanowire field effect transistor sensors.* Nano Letters, 2007. **7**(11): p. 3405-3409.
5. Heller, I., et al., *Identifying the mechanism of biosensing with carbon nanotube transistors.* Nano Letters, 2008. **8**(2): p. 591-595.
6. Stern, E., et al., *Label-free immunodetection with CMOS-compatible semiconducting nanowires.* Nature, 2007. **445**(7127): p. 519-522.
7. Elfstrom, N., A.E. Karlstrom, and J. Linnros, *Silicon nanoribbons for electrical detection of biomolecules.* Nano Letters, 2008. **8**(3): p. 945-949.

8. Aroonyadet, N., et al., *Highly scalable, uniform, and sensitive biosensors based on top-down indium oxide nanoribbons and electronic enzyme-linked immunosorbent assay.* Nano Letters, 2015. **15**(3): p. 1943-51.

9. Liu, Q., et al., *Highly Sensitive and Quick Detection of Acute Myocardial Infarction Biomarkers Using In2O3 Nanoribbon Biosensors Fabricated Using Shadow Masks.* ACS Nano, 2016. **10**(11): p. 10117-10125.

10. Minot, E.D., et al., *Carbon nanotube biosensors: The critical role of the reference electrode.* Applied Physics Letters, 2007. **91**(9).

11. Lewandrowski, K., A. Chen, and J. Januzzi, *Cardiac markers for myocardial infarction. A brief review.* Am J Clin Pathol, 2002. **118 Suppl**: p. S93-9.

12. Qureshi, A., Y. Gurbuz, and J.H. Niazi, *Biosensors for cardiac biomarkers detection: A review.* Sensors and Actuators B: Chemical, 2012. **171–172**(0): p. 62-76.

13. Kong, T., et al., *CMOS-compatible, label-free silicon-nanowire biosensors to detect cardiac troponin I for acute myocardial infarction diagnosis.* Biosens Bioelectron, 2012. **34**(1): p. 267-72.

14. Lee, I., et al., *Detection of Cardiac Biomarkers Using Single Polyaniline Nanowire-Based Conductometric Biosensors.* Biosensors, 2012. **2**(2): p. 205-220.

15. Zhang, G.-J., et al., *An integrated chip for rapid, sensitive, and multiplexed detection of cardiac biomarkers from fingerprick blood.* Biosensors and Bioelectronics, 2011. **28**(1): p. 459-463.

16. Chua, J.H., et al., *Label-free electrical detection of cardiac biomarker with complementary metal-oxide semiconductor-compatible silicon nanowire sensor arrays.* Anal Chem, 2009. **81**(15): p. 6266-71.

17. Zhang, G.-J., et al., *Multiplexed detection of cardiac biomarkers in serum with nanowire arrays using readout ASIC.* Biosensors and Bioelectronics, 2012. **35**(1): p. 218-223.

18. Jo, K., H.Z. Yu, and H. Yang, *Formation kinetics and stability of phosphonate self-assembled monolayers on indium-tin oxide.* Electrochimica Acta, 2011. **56**(13): p. 4828-4833.

19. Gao, X.P.A., G.F. Zheng, and C.M. Lieber, *Subthreshold Regime has the Optimal Sensitivity for Nanowire FET Biosensors*. Nano Letters, 2010. **10**(2): p. 547-552.

20. Stern, E., et al., *A nanoelectronic enzyme-linked immunosorbent assay for detection of proteins in physiological solutions*. Small, 2010. **6**(2): p. 232-8.

21. Mahajan, V.S. and P. Jarolim, *How to interpret elevated cardiac troponin levels*. Circulation, 2011. **124**(21): p. 2350-4.

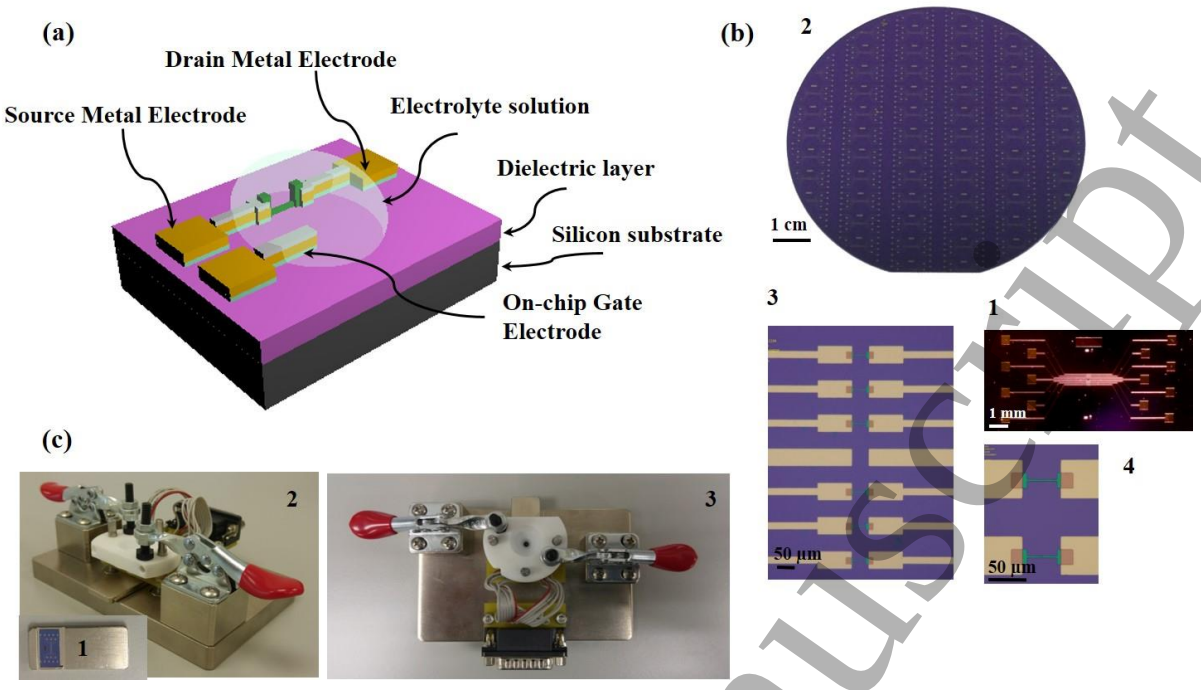

Figure 1 (a) Device schematic diagram (b-1) Fabricated biosensor chips on a 3 inch Si wafer with 300 nm SiO_2 dielectric layer (b-2) an In_2O_3 nanoribbon FET biosensor chip has 6 transistors and 2 on-chip gate electrodes (b-3) a magnified photo of a chip (b-4) nanoribbons in the active area bridged between source and drain metal electrodes (c-1) a chip tray where we place a FET chip before we put under a Teflon taper shape cell for the biosensing experiment (c-2) a side view of the test fixture after we inserted the chip tray and press both clamp down for sealing solution during sensing experiments. (c-3) a top-view image of a test fixture used for biosensing experiments to confine solution on top of the In_2O_3 nanoribbon FETs.

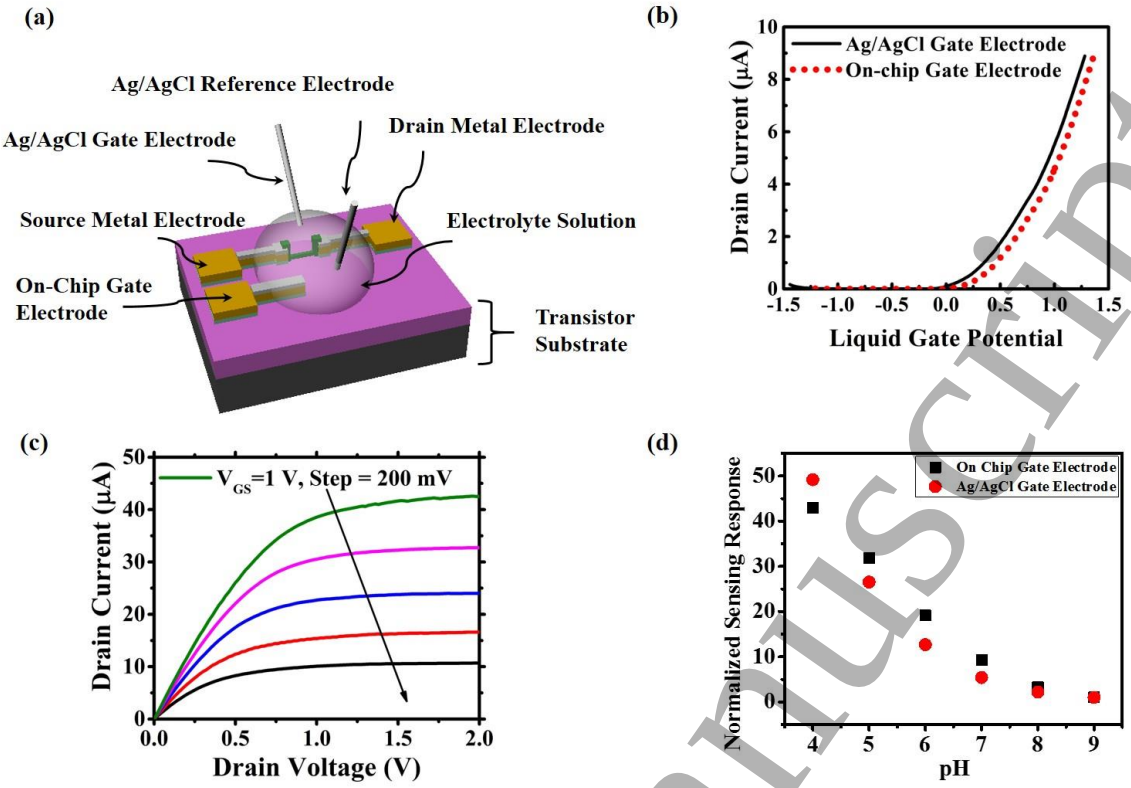

Figure 2 (a) Liquid gate measurement schematic diagram (b) A performance comparison between a transistor biased through a Ag/AgCl electrode and an on-chip gate electrode (c) A family of drain current and drain voltage ($I_{DS} - V_{DS}$) of an In_2O_3 nanoribbon FET when the liquid gate potential was applied through an on-chip gate electrode (d) A comparison of average pH sensing responses when sensors biased by a Ag/AgCl gate electrode and an on-chip gate electrode

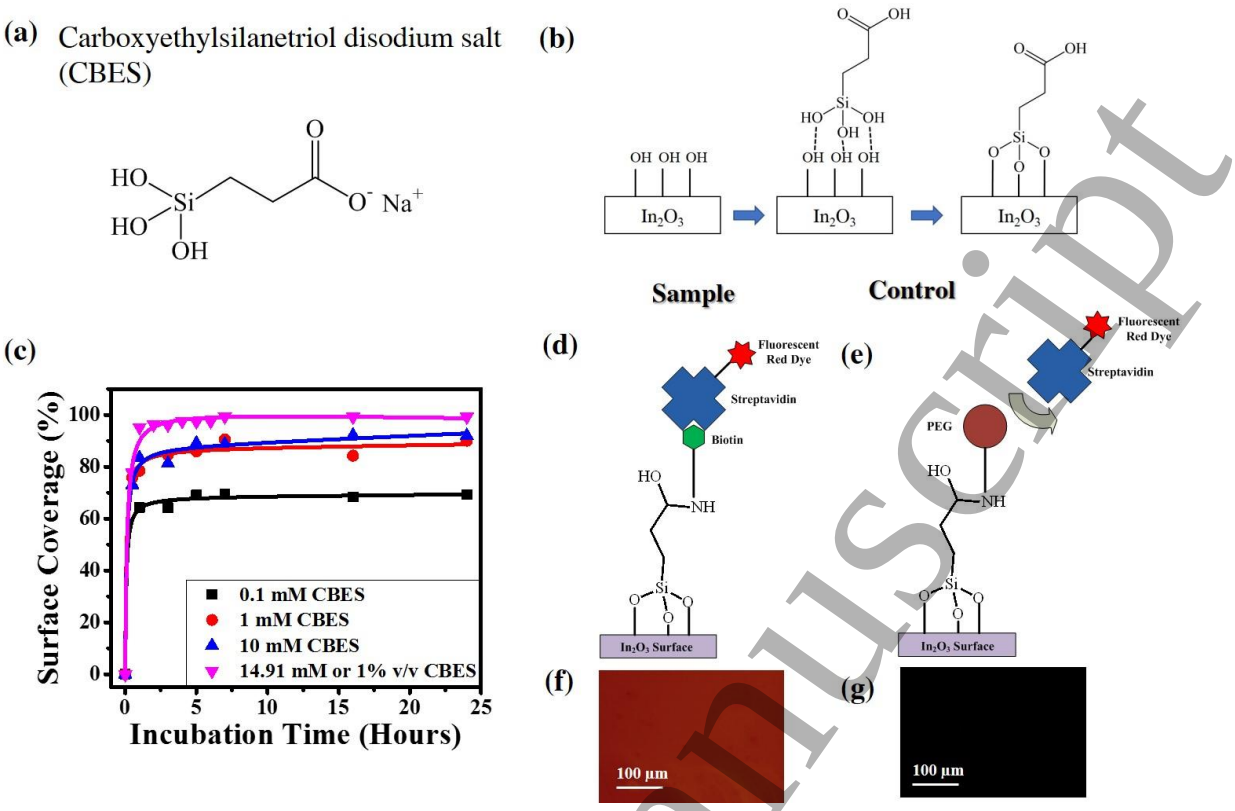

Figure 3 (a) A chemical structure of a carboxyethylsilanetriol (CBES) linker molecule (b) Schematic diagrams of CBES functionalization on the surface of indium oxide surface (c) A relationship between surface coverage calculated and measured using electrochemical impedance spectroscopy (EIS) on indium tin oxide (ITO) surface as model of this study at concentration of 0.1 mM , 1 mM , 10 mM and 14.91 mM or 1% v/v CBES solution with varying incubation times from 30 minutes to 24 hours (d) and (e) Diagrams of the fluorescent experiment to validate the coverage of CBES molecules on the metal oxide surface at 1 hour incubation time on the indium oxide film for a sample substrate and its negative control substrate, respectively (f) and (g) Fluorescent photographs of the sample substrate and its negative control as the experiment in diagrams in (d) and (e), respectively.

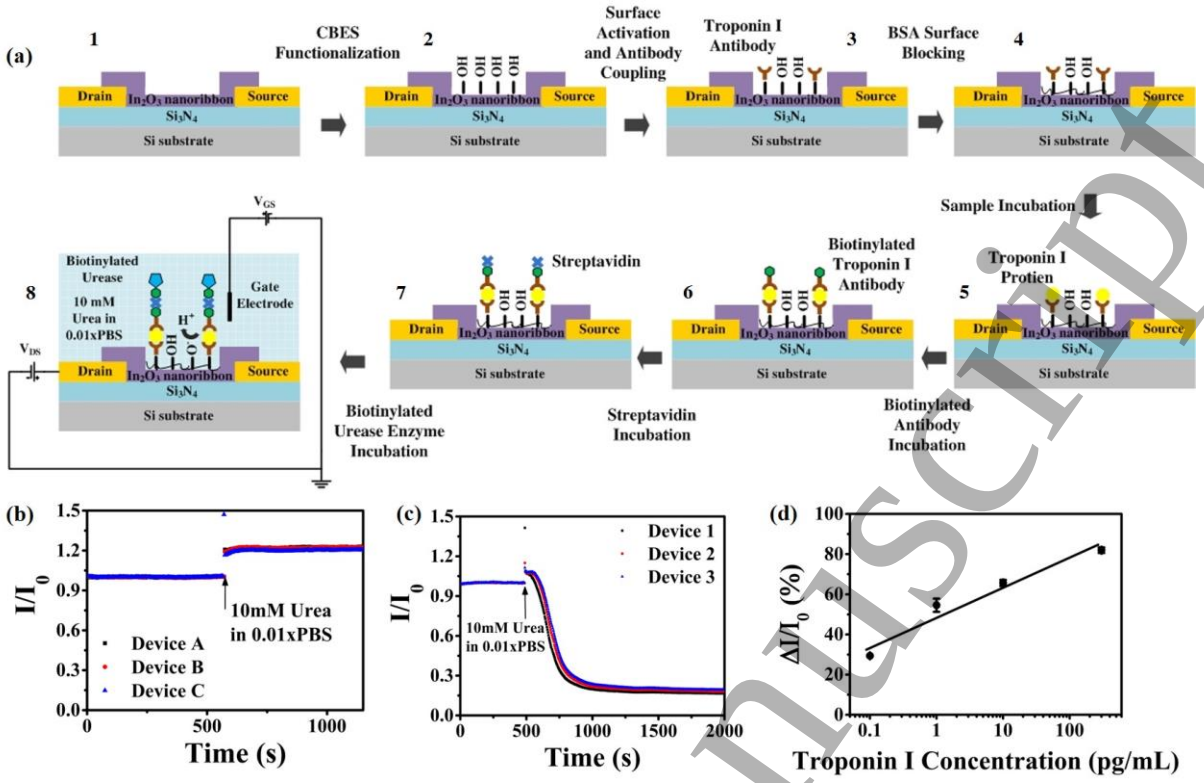

Figure 4 (a) Schematic diagrams of surface modification on an In_2O_3 nanoribbon FET chip for the detection of troponin I protein by the electronic ELISA technique. (a-1) and (a-2) A clean nanoribbon chip was functionalized to anchor CBES molecules on the surface of nanoribbons. (a-3) CBES molecules on the In_2O_3 surface were activated by EDC/NHS chemistry to immobilize troponin I antibodies. (a-4) The surface of nanoribbons was blocked by BSA protein to prevent unspecific binding of biomolecules. (a-5) The troponin I protein in the sample was captured by troponin I antibodies while other unbound proteins were washed off from the device surface. (a-6) Biotinylated troponin I antibodies were anchored on top of immobilized troponin I proteins. (a-7) The streptavidin was captured on the biotin terminal of the biotinylated troponin I antibody. (a-8) Urease enzymes were bound to streptavidin molecules on nanoribbons and the number of enzymes corresponds to the concentration of troponin I protein in the sample. (b) and (c) Real time sensing responses of 3 fabricated In_2O_3 nanoribbon FET biosensors toward troponin I cardiac biomarker at 300 pg/mL concentration without and with biotinylated urease enzymes in the sensing chamber, respectively. Devices were biased by an on-chip gate electrode while performing the experiment. (d) A plot of average normalized sensing

responses and their standard deviation from 3 devices at each troponin I concentration in picograms per milliliter.